Antiviral Research 80 (2008) 23–35

Contents lists available at ScienceDirect

Antiviral Research

journal homepage: www.elsevier.com/locate/antiviral

Review

The flavivirus polymerase as a target for drug discovery

Hélène Malet[a,1], Nicolas Massé[a,1], Barbara Selisko[a], Jean-Louis Romette[a], Karine Alvarez[a], Jean Claude Guillemot[a], Hughes Tolou[b], Thai Leong Yap[c,d], Subash Vasudevan[d], Julien Lescar[a,c,d], Bruno Canard[a,*]

[a] *Architecture et Fonction des Macromolécules Biologiques, CNRS and Universités d'Aix-Marseille I et II, UMR 6098, ESIL Case 925, 13288 Marseille, France*
[b] *Institut de Médecine Tropicale du Service de Santé des Armées, Le Pharo, Avenue Charles Livon, 13007 Marseille, France*
[c] *School of Biological Sciences, Nanyang Technological University, 60 Nanyang Drive, Singapore 637551, Singapore*
[d] *Novartis Institute for Tropical Diseases, 10 Biopolis Road, Chromos Building, Singapore 138670, Singapore*

ARTICLE INFO

Article history:
Received 11 April 2008
Accepted 10 June 2008

Keywords:
Dengue virus
West Nile virus
Flavivirus
RNA-dependent RNA polymerase
De novo
Drug design
Crystal structure

ABSTRACT

Flaviviruses are emerging pathogens of increasingly important public health concern in the world. For most flaviviruses such as dengue virus (DENV) and West Nile virus (WNV) neither vaccine nor antiviral treatment is available. The viral RNA-dependent RNA polymerase (RdRp) non-structural protein 5 (NS5) has no equivalent in the host cell and is essential for viral replication. Here, we give an overview of the current knowledge regarding *Flavivirus* RdRp function and structure as it represents an attractive target for drug design. *Flavivirus* RdRp exhibits primer-independent activity, thus initiating RNA synthesis *de novo*. Following initiation, a conformational change must occur to allow the elongation process. Structure-function studies of *Flavivirus* RdRp are now facilitated by the crystal structures of DENV (serotype 3) and WNV RdRp domains. Both adopt a classic viral RdRp fold and present a closed pre-initiation conformation. The so-called priming loop is thought to provide the initiation platform stabilizing the *de novo* initiation complex. A zinc-ion binding site at the hinge between two subdomains might be involved in opening up the RdRp structure towards a conformation for elongation. Using two different programs we predicted common potential allosteric inhibitor binding sites on both structures. We also review ongoing approaches of *in vitro* and cell-based screening programs aiming at the discovery of nucleosidic and non-nucleosidic inhibitors targeting *Flavivirus* RdRps.

Contents

Abbreviations: BVDV, bovine viral diarrhea virus; CS, cyclization sequences; DENV, dengue virus; ds, double strand; HCV, hepatitis C virus; HTS, high-throughput screening; MTase, methyltransferase; NI, nucleoside analogue inhibitors; NLS, nuclear localization sequence; NNI, non-nucleoside analogue inhibitors; RdRp, RNA-dependent RNA polymerase; RF, replicative form; RI, replicative intermediate; ss, single strand; tP, triphosphate; TR, terminal regions; WNV, West Nile virus; YFV, yellow fever virus.

* Corresponding author.
E-mail address: Bruno.Canard@afmb.univ-mrs.fr (B. Canard).

[1] These authors contributed equally to this work.

0166-3542/$ – see front matter © 2008 Elsevier B.V. All rights reserved.
doi:10.1016/j.antiviral.2008.06.007

1. Introduction

Members of the genus *Flavivirus* in the family *Flaviviridae* cause some of the most important examples of emerging diseases, exemplified by the increasing prevalence of dengue virus (DENV) in the tropical and subtropical areas of the world, the emergence of West Nile virus (WNV) in North America, and the spread of Japanese encephalitis virus (JEV) through much of Asia and into Oceania. Currently, there are only three vaccines against *Flavivirus* infections: that of yellow fever virus (YFV), JEV and tick-borne encephalitis virus (TBEV), but they have met with limited success to contain epidemics (Pugachev et al., 2003; Mackenzie et al., 2004). The long-awaited development of a vaccine against dengue is hampered by the existence of four serotypes DENV1 to DENV4 (Chaturvedi et al., 2005; Whitehead et al., 2007). Currently, no antiviral drug is available against any *Flavivirus* infection. The *Flavivirus* RNA-dependent RNA polymerase (RdRp) is considered one of the most interesting targets for drugs since polymerase activity is essential for viral replication, and human host cells are devoid of such RdRp (Cerutti and Casas-Mollano, 2006). The clinical use of inhibitors against the HIV reverse transcriptase, the hepatitis B virus polymerase and the herpes virus polymerase has validated viral polymerases as therapeutic targets (De Clercq, 2005). Inhibitors of the RdRp of hepatitis C virus (HCV), belonging to the genus *Hepacivirus* of the family *Flaviviridae*, are currently undergoing clinical trials (De Francesco and Carfi, 2007). Here, we review the current knowledge on *in vivo* and *in vitro* characterization of *Flavivirus* RdRp activity, the recently described crystal structures of DENV and WNV RdRps, and finally the drug discovery efforts directed against *Flavivirus* polymerase and replication.

2. Flavivirus replication and the discovery of NS5-mediated RdRp activity

Flaviviruses contain a single-strand (ss) positive sense RNA genome, which bears a type-1 cap-structure ($^{7Me}GpppA_{2'OMe}$) at the 5′ end and no poly(rA) tail at the 3′end except for some TBEV strains (Mandl et al., 1991). Upon infection, the viral genomic RNA acts as mRNA, which is translated to a large polyprotein encompassing structural and non-structural proteins (NS1–5), the latter constituting the replicative complex. RNA replication involves synthesis of complementary minus strands that are then used as templates for the production of plus strands (see schema in Fig. 1). From RNA labelling experiments using Kunjin virus (Australian subtype of WNV), Chu and Westaway (Chu and Westaway, 1985) proposed that *Flavivirus* RNA synthesis occurs through an asymmetric replication cycle. Ten times more plus strand (+) than minus strand (−) is synthesized in *Flavivirus*-infected cells. Three main forms of viral RNA have been detected: a ss genomic RNA of positive sense (40–44 S), a double strand (ds) replicative form (RF; 20–22 S), and partially ss replicative intermediates (RI; heterogeneous 20–28 S) (Cleaves et al., 1981; Chu and Westaway, 1985). Both RF and RI are intermediates in the synthesis of genomic RNA and interconvert to each other in a cyclic manner. (+) RNA synthesis is taking place at the RF in a semi-conservative fashion. Neosynthesized (+) RNA displaces the old RNA. (+) RNA can finally be used for further translation, minus strand synthesis or be encapsidated into virions. Conserved sequence motifs within the C-terminal part of *Flavivirus* NS5 had suggested that this protein, which comprises in full around 900 amino acids, is the RdRp (Rice et al., 1985; Poch et al., 1989; Bruenn, 1991; Koonin, 1991). This was finally demonstrated by the use of NS5-specific antisera that inhibited RdRp activity in assays using DENV2 infected cell lysates (Bartholomeusz and Wright, 1993), as well as DENV1 recombinant RdRp (Tan et al., 1996).

3. Molecular characterization of the RdRp enzymatic activity of *flavivirus* NS5

An *in vitro* assay for *Flavivirus* RdRp activity was established using extracts of Vero cells infected with DENV2 or WNV (Bartholomeusz and Wright, 1993) where RNA synthesis was triggered by exogenous viral RF. It was shown that RF was converted to RI. The first report of an active recombinant *Flavivirus* RdRp was that of DENV1 NS5 expressed in *E. coli* as a GST fusion. It bound RNA template and showed RdRp activity as detected by the incorporation of radiolabel into a neosynthesized RNA strand (Tan et al., 1996). NS5 RdRp of flaviviruses has now been expressed in various *in vitro* systems, and shown to have RdRp activity (Tan et al., 1996; Ackermann and Padmanabhan, 2001; Guyatt et al., 2001; Nomaguchi et al., 2003; Nomaguchi et al., 2004; Selisko et al., 2006). To elucidate the mechanism of viral replication at the molecular level, various *in vitro* RdRp assays have been developed. Homopolymeric or heteropolymeric, *in vitro* transcribed, RNA templates that may contain specific and essential regulatory elements of the viral genome have been used.

3.1. Flavivirus RdRp initiates RNA synthesis de novo

You and Padmanabhan (You and Padmanabhan, 1999) observed that two RNA products were formed using a subgenomic DENV2 RNA template containing both 5′ and 3′ terminal regions (TR) upon incubation with cytoplasmic extracts from DENV2 infected mosquito cells. One product had the same mobility and size as the input RNA template. The second product showed a faster mobility on a partially denaturing polyacrylamide gel containing 7 M urea. Under more stringent denaturing conditions, the second product was consistent with a size twice that of the template RNA. The latter product was converted to a product with the same mobility as the template RNA upon digestion with RNase A. These results suggested

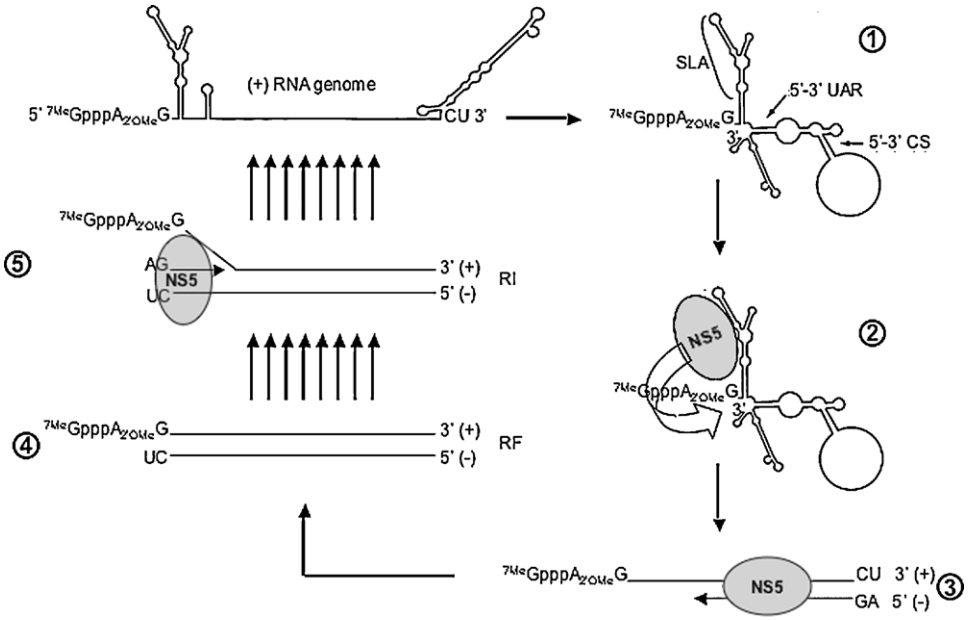

Fig. 1. Schema of *Flavivirus* RNA replication. Capped genomic (+) RNA is circularized (1) due to interactions between complementary sequence stretches at the 5′ and 3′ ends named UAR (Upstream of AUG Region) and CS (complementary sequences). The NS5 RdRp domain specifically binds to the promoter stem loop A (SLA) at the 5′ end of the genome and initiates *de novo* RNA synthesis using the 3′ end as a template (2). The NS5 RdRp synthesizes the complete (−) strand (3). The double-stranded RNA replicative form (RF), consisting of the genomic strand annealed to the neosynthesized (−) strand (4), serves as a template for the synthesis of new genomic (+) RNA, in the replicative intermediate (RI) (5). Figure was adapted from Filomatori et al. (2006).

that it was a ds hairpin RNA, with a short ss loop region. The hairpin species seemed to be formed by a 'copy back' mechanism. Elongation of the 3′ end of the template takes place due to intramolecular priming where the 3′ end anneals to a complementary sequence stretch of the RNA template. These two RNA products, the ss template size and the ds hairpin have also been observed in other studies using purified NS5, without any detectable traces of contaminating nucleases (Steffens et al., 1999; Ackermann and Padmanabhan, 2001; Nomaguchi et al., 2004; Selisko et al., 2006). Thus, the template size product was not generated by the digestion of the hairpin RNA product by a nuclease present in the crude or purified extract of infected cells but by *de novo* (i.e. primer-independent) initiation of RNA synthesis. More evidence for *de novo* initiation was provided by the fact that on DENV2 and WNV subgenomic RNA templates with blocked 3′ ends only template size products were formed (Ackermann and Padmanabhan, 2001; Nomaguchi et al., 2004). Accordingly, DENV2 or WNV NS5 generated a poly(rG) product in absence of a primer on homopolymeric poly(rC) templates (Selisko et al., 2006). Thus, *Flavivirus* RdRps are primer-independent polymerases, able to initiate RNA synthesis *de novo*.

Based on these observations, the lack of evidence of formation of copy back products *in vivo* (Chu and Westaway, 1985) and in analogy to *de novo* replication strategies of other related viruses of the *Flaviviridae* family such as HCV (Oh et al., 1999; Luo et al., 2000; Zhong et al., 2000) and the pestivirus bovine viral diarrhea virus (BVDV) (Kao et al., 1999), it is expected that the *de novo* initiation of RNA synthesis corresponds to the RNA replication strategy adopted by *Flavivirus* RdRps *in vivo*. The hairpin product seems to remain an *in vitro* artefact, which nevertheless allowed making valuable hypotheses about the manner in which the RdRp initiates and pursues RNA synthesis (see Section 3.4).

3.2. Definition of the Flavivirus RdRp domain and characterization of its de novo RdRp activity

Full-length NS5 of around 900 amino acids bears a methyltransferase (MTase) activity in the N-terminal part of the protein involved in RNA cap formation (Egloff et al., 2002; Ray et al., 2006,see Chapter NS5 MTase in this issue), two functional nuclear localization sequences bNLS and a/bNLS comprising DENV2 residues 320–368 and 369–389 (Brooks et al., 2002; Pryor et al., 2007) and the RdRp motifs in the C-terminal part (Rice et al., 1985; Poch et al., 1989; Bruenn, 1991; Koonin, 1991). The NLS region has long been thought erroneously to represent a linker between the two domains (see below). Structure-based sequence analysis of NS5 in comparison with the known 3D structures of the RdRps of HCV and BVDV allowed the definition and subsequent production of a recombinant soluble and enzymatically active RdRp domain of DENV2 and WNV starting at DENV2 NS5 residue 272 (Selisko et al., 2006). A comparison of steady-state enzymatic activity parameters of both full-length NS5 and RdRp domains on a homopolymeric template poly(rC) suggested that the MTase domain does not influence *de novo* RdRp activity (Selisko et al., 2006). This indicates that the RdRp domain alone can be used for screening processes and characterization of inhibitors of the *Flavivirus* RdRp activity.

3.3. Flavivirus RdRp domain interacts simultaneously with 3′ and 5′ terminal regions of genomic template RNA

The 5′ and 3′ TR of the *Flavivirus* RNA genome contain complementary 5′ and 3′ cyclization sequences (CS) and a 3′ terminal stem loop structure that have been shown to be important for RNA synthesis *in vitro* using DENV2-infected cell lysates (You and Padmanabhan, 1999; You et al., 2001). These structures are also essential for viral RNA replication in cultured cells, as shown by mutagenesis of infectious DENV2 RNA (Zeng et al., 1998) as well as WNV (Khromykh et al., 2001; Lo et al., 2003) and YFV (Corver et al., 2003) replicon RNA. Accordingly, purified recombinant DENV2 NS5 protein is active in the synthesis of the (−) RNA from (+) subgenomic RNA templates containing intact CS stretches but not from an RNA containing only the 3′ TR (Ackermann and Padmanabhan, 2001). Recently additional complementary sequence stretches at the 5′ and 3′ end of DENV genomic RNA named UAR (Upstream of

AUG Region), whose interaction was important for DENV2 replication, were identified (Alvarez et al., 2005). Additionally in the same study the physical interaction of the 5′ and 3′ ends of DENV2 genome leading to its cyclization was actually shown by atomic force microscopy (AFM). More recently, it has been shown by AFM that the RdRp domain of DENV2 binds to circular RNA genome and that *de novo* RNA synthesis of the negative strand is enhanced by the presence of a promoter element, a large stem-loop structure named SLA present at the 5′ end of the genome (Filomatori et al., 2006). The authors demonstrated the physical interaction of the RdRp domain with SLA and subsequently proposed a novel mechanism for (−) RNA synthesis in which the *Flavivirus* RdRp specifically binds SLA at the 5′ end of the genome. It then reaches the site of initiation at the 3′ end recruited to the 5′ end via long-range RNA–RNA interactions. The disruption of the interaction between RdRp domain and SLA constitutes thus an additional approach towards the development of anti-flavivirus agents.

In contrast to (−) RNA synthesis, the presence of the 3′ TR of the (−) RNA template alone seems to be sufficient for (+) RNA synthesis. Neither the minus strand 5′ end nor the 3′ CS motif were essential for (+) RNA synthesis (Nomaguchi et al., 2004). In the infected cell *Flavivirus* (−) RNA synthesis is thought to proceed from the RF form (Chu and Westaway, 1985), where (+) and (−) RNA are annealed. This places the 5′ SLA of the (+) RNA, potentially formed upon the initial dissociation of the two strands, near the 3′ end of (−) RNA perhaps further facilitating the recruitment of the RdRp domain to its starting point. Further studies are awaited to shed more light on the mechanistic details of *Flavivirus* RNA replication.

3.4. Initiation and elongation phases of RNA synthesis may involve the RdRp domain adopting two different conformational states

In a DENV2 RdRp assay with subgenomic template and full-length NS5, the ratio between *de novo* and hairpin products was shown to be directly dependent on the temperature. The template size *de novo* initiation product was predominantly formed at temperatures under 30° whereas at higher temperatures a predominance of hairpin product was observed (Ackermann and Padmanabhan, 2001) (Fig. 2). The use of just three NTPs in the initial phase of RNA synthesis and subsequent trapping of free RdRp allowed the experimental dissociation of initiation from elongation of RNA synthesis. It was shown that the temperature gradient for initiation events resembled the temperature dependence for the formation of the *de novo* template size product. There was no difference in the relative amounts of *de novo* and hairpin product when the elongation phase was subjected to different temperatures (Ackermann and Padmanabhan, 2001). A model was proposed in which DENV2 RdRp enzyme assumes two different conformational stages during initiation and elongation, a more rigid 'closed' conformation at low temperature favoring initiation and a more mobile 'open' conformation at higher temperature favoring elongation. Additionally, utilization of synthetic primers by NS5 indicated that the tetranucleotide AGAA is the optimal primer for elongation, whereas AG, AGA and AGAACC were inefficient primers (Nomaguchi et al., 2003). Thus, a complete model consistent with these results is that active site of the polymerase switches from a 'closed' form, catalyzing *de novo* initiation through synthesis of short primers (up to four nucleotides), to an 'open' form for elongation. Such a model of a conformational change between initiation and elongation is supported by assays on homopolymeric poly(rC) or oligo$(rC)_{15}$ templates using the RdRp domains of DENV2 and WNV NS5, in which abortive products GG and, to a lesser extent, GGGG accumulate during the reaction indicating a rate-limiting conformational change marking the transition between initiation

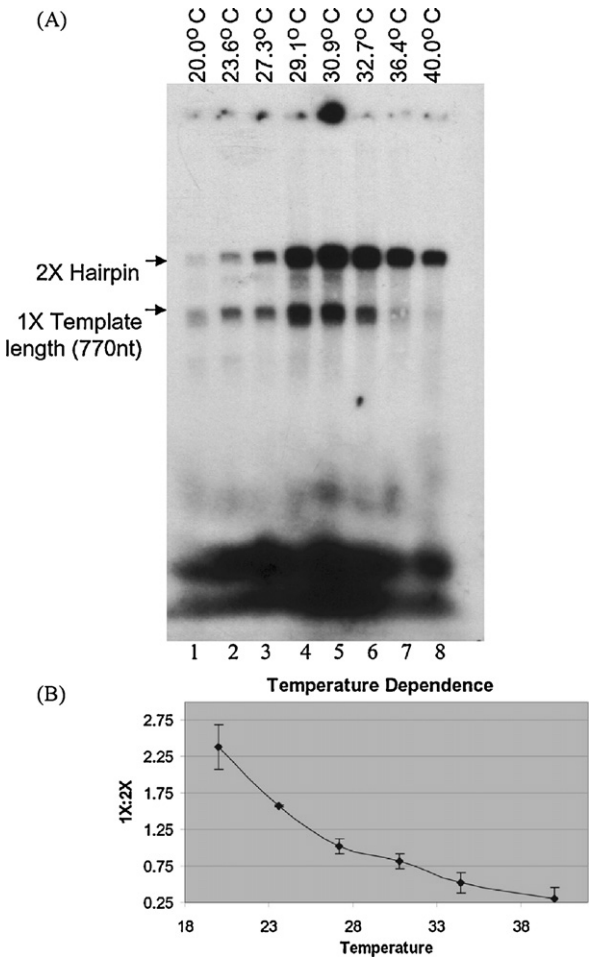

Fig. 2. *De novo* RNA synthesis by DENV2 NS5 is temperature-dependent. (A) Purified NS5 was incubated with subgenomic RNA for 90 min at varying temperatures as described in Ackermann and Padmanabhan (2001). Products were resolved by fully denaturating formaldehyde-agarose gel electrophoresis and subjected to autoradiography. (B) Bands were excised from dried gel and subjected to liquid scintillation counting. The average ratio of *de novo* (1×) to 3′ end elongation (2×) products from three separate experiments were plotted. Figure was reproduced with permission from Ackermann and Padmanabhan (2001).

and elongation (Selisko et al., 2006; Fig. 3). For HCV RdRp several inhibitors have been identified that bind to the enzyme in a similarly closed initiation conformation thus preventing the putative conformational change towards elongation (De Francesco and Carfi, 2007). In analogy to HCV RdRp, one mechanism of a future efficient *Flavivirus* RdRp inhibitor could be the trapping of the enzyme in its initiation state. Interestingly, the extent of the accumulation of abortive products by WNV RdRp was much higher than for DENV2 RdRp (Fig. 3). In this sense WNV RdRp resembles much more HCV RdRp for which strong accumulation of short abortive products has been shown (Fig. 3).

4. Crystal structure of the RdRp domains of *Flavivirus* NS5

4.1. RdRp domain structure determination

The structural characterization of *Flavivirus* RdRp enzyme has long been hampered by the difficulty either to obtain important amounts of pure recombinant protein due to the instability of full-length NS5 or to delineate the N-terminal start of a putatively soluble RdRp domain (see Section 3.2). Finally, enzymatically active RdRp domains of DENV and WNV NS5 were successfully delineated,

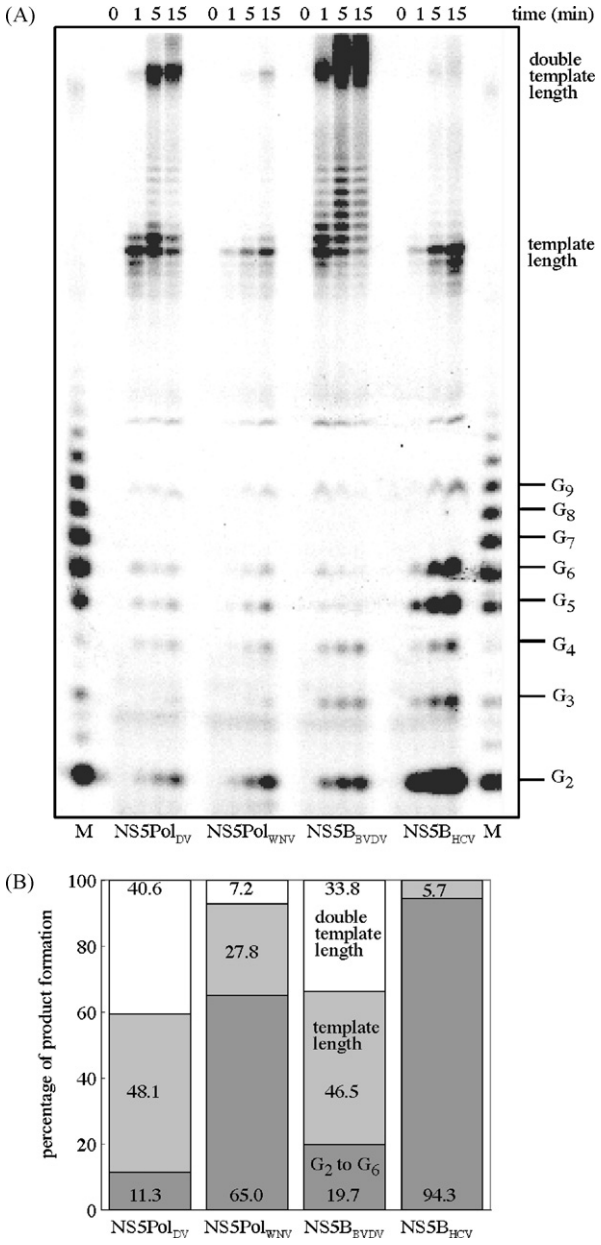

Fig. 3. *De novo* RNA synthesis by NS5Pol$_{DV}$, NS5Pol$_{WNV}$, NS5B$_{BVDV}$ and NS5B$_{HCV}$ using an oligo(rC) RNA template. Reaction mixtures containing 400 nM enzyme, 10 μM oligo(rC) and 100 μM [α-^{32}P]-GTP were set up and processed as described in (Selisko et al., 2006). Reaction time course was followed up to 15 min. (A) RNA products were resolved on a 14% polyacrylamide gel containing 7 M urea. M: Oligo(rG) RNA synthesized by T7 DdRp was used as RNA size marker. The identity of each band is indicated on the right. (B) Percentage of abortive, template-length and double-template length products upon *de novo* RNA synthesis. Product bands were quantitated and the percentage of GMP incorporation in each product calculated from relative intensities of the corresponding band. Figure was taken from Selisko et al. (2006).

expressed and purified in high yield relative to full length NS5 (Selisko et al., 2006). Crystallogenesis using commercial screens and optimization allowed eventually the determination of structures of both WNV and DENV3 RdRps (Malet et al., 2007; Yap et al., 2007). Crystal structures of nine viral RdRps had been reported before (reviewed in Ferrer-Orta et al., 2006). In the *Flaviviridae* family, the genera *Hepacivirus* (HCV RdRp) and *Pestivirus* (BVDV RdRp) were represented (Ago et al., 1999; Bressanelli et al., 1999; Lesburg et al., 1999; Choi et al., 2004). The low sequence identity of *Flavivirus* RdRps compared to other RdRps with existing structures (20% structural identity between HCV, BVDV and WNV/DENV3 RdRps) precluded the use of the molecular replacement method. As a first step in *Flavivirus* RdRp structure determination, the structure of a shorter form of the WNV RdRp domain (strain Kunjin comprising the residues 317–905) could be solved using single anomalous dispersion at 2.35 Å resolution. This form of WNV RdRp then allowed structure determination of longer forms (comprising the residues 273–905) of WNV RdRp (3 Å resolution) and DENV3 RdRp (1.85 Å resolution). These latter constructs were shown to be enzymatically active whereas the shorter form was not (Malet et al., 2007; Yap et al., 2007).

4.2. Overall structure

Both WNV and DENV3 RdRps adopt a typical RdRp right-hand structure comprising three subdomains: fingers, palm and thumb (Fig. 4). Their fold is analogous with an RMSD of 1.9, 0.8 and 1.0 Å for the fingers, palm and thumb, respectively. They display a closed conformation, characteristic of RdRps and in particular of primer-independent (*de novo*) RdRps (reviewed in Ferrer-Orta et al., 2006). One of the fingertips protrudes from the fingers subdomain and connects to the thumb. A structural element, named the priming loop, provides the initiation platform. It points from the thumb subdomain towards the active site in the palm (see below). The active site is located at the intersection of two tunnels. Other RdRps solved in complex with RNA template, NTPs and/or ds RNA product (Huang et al., 1998; Butcher et al., 2001; Ferrer-Orta et al., 2007) suggest the following scenario, shown in Fig. 4. The first tunnel, located between the fingers and the thumb, should allow the ss RNA template to access the active site. The second tunnel, roughly perpendicular to the first, goes across the entire protein. The incoming NTP should arrive from the back of the tunnel and, after the polymerization has started, the nascent ds RNA should go out through the front of this tunnel. However, as for other *de novo* RdRps a conformational change is necessary to avoid a steric clash with the priming loop (see below) and allow neo-synthesized ds RNA to exit.

4.3. The palm subdomain

The palm subdomain contains the active site and constitutes the structurally most conserved subdomain among all known polymerases. In the *Flavivirus* RdRps it is composed of two anti-parallel β-strands surrounded by 8 α-helices. It contains three functional motifs involved in RNA synthesis. In particular, two aspartic acids (Fig. 5A) belonging to motif A (aa 533 in DENV3) and motif C (aa 663) have been shown to play a role in the catalytic mechanism (Steitz, 1998; Butcher et al., 2001; Tao et al., 2002; Castro et al., 2007). Aspartate 533 acts as a general base and deprotonates the 3′ hydroxyl group of the priming NTP, which subsequently attacks the α-phosphate of the NTP to be incorporated. The aspartate 663 promotes a suitable geometry for the reaction to occur. These aspartates also coordinate the metal ions involved in catalysis. No catalytic ion has been observed in the *Flavivirus* RdRps structures. However, a magnesium ion in a non-catalytic position is found in both catalytically active *Flavivirus* RdRp structures. Moreover, the shorter construct of WNV contains a calcium ion (known to inhibit the polymerization reaction) in the same non-catalytic position. The role of the non-catalytic ion is still elusive. It was proposed that it might play a role in the *de novo* initiation mechanism facilitating the movement of the nascent ds RNA after formation of the first dinucleotide out of the active site (Butcher et al., 2001). It is coordinated by aspartic acids 533 and 664. As Asp-533 is involved in the coordination of the catalytic magnesium ion, a conformational change of its side chain is required to allow the polymerase to initiate polymerization.

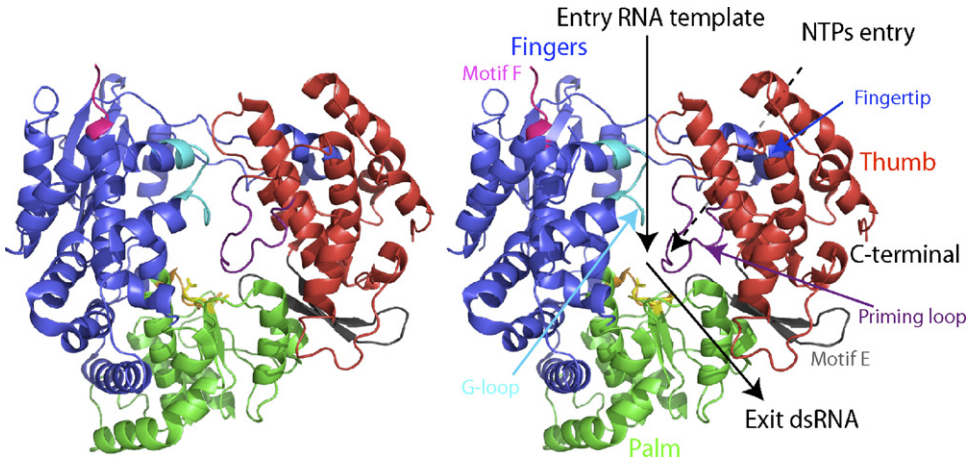

Fig. 4. WNV RdRp overall structure. "Front" view of WNV RdRp in ribbon representation. Fingers, palm and thumb subdomains are colored in blue, green and red, respectively. The ss RNA template entry and the ds RNA exit are shown by black arrows. A dotted arrow points to the NTP entry tunnel at the back of the RdRp. Motifs A, C, E, F, the G-loop and the priming loop are colored in orange, yellow, grey, magenta, cyan and purple, respectively. The aspartic acids of the motifs A and C (Asp-533, Asp-663 and Asp-664) are represented in sticks. (For interpretation of the references to color in this figure legend, the reader is referred to the web version of the article.)

4.4. *The fingers subdomain*

The fingers subdomain is composed of a core and two fingertips (Fig. 4). The core of the fingers subdomain forms a three-stranded β-sheet absent in the structures of HCV and BVDV RdRps. The integrity of this β-sheet is required for activity. The absence of its first β-strand in the short WNV RdRp construct leads presumably to the disorder of the β-sheet and destabilization of the

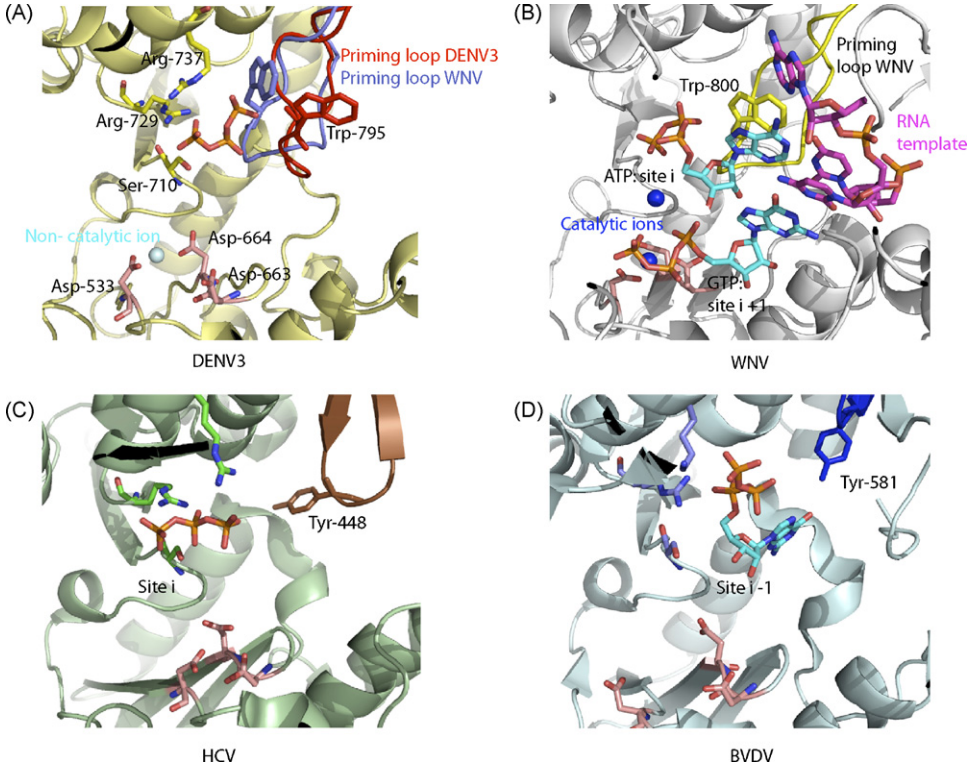

Fig. 5. Nucleotide complexes of DENV3, HCV, BVDV RdRps and *de novo* initiation model of WNV RdRp. (A) DENV3 RdRp is shown in yellow ribbon. The triphosphate of 3′dGTP is represented in sticks (phosphate in orange, oxygen in red). Residues coordinating it in DENV3 RdRp are represented by sticks and colored according to atom types (carbon in yellow, phosphate in orange, oxygen in red, nitrogen in blue). Corresponding residues in HCV and BVDV RdRps are colored in green and blue sticks respectively in (C) and (D). The DENV3 RdRp priming loop is shown in red and can be compared to the one of WNV RdRp shown in blue. The residues of the priming loop putatively involved in the stabilization of the initiation complex, namely Trp-795 in DENV3 and Trp-800 in WNV RdRp, are represented with red and blue sticks, respectively. Catalytic aspartic acids are represented by pink sticks and the non-catalytic ion by a light blue sphere. (B) Initiation model of WNV RdRp in the same orientation as in (A). The RNA template and NTPs to be incorporated are shown in magenta and cyan sticks, respectively. The priming loop is shown in yellow ribbon with the proposed initiation-platform residue Trp-800 in yellow sticks. Catalytic ions are represented by blue spheres and the catalytic aspartic acids are shown in light pink sticks. (C) HCV RdRp is shown in green ribbon (in the same orientation as the *Flavivirus* RdRps in (A)). The triphosphate of dUTP bound in site *i* is represented by sticks. The priming loop is shown in brown ribbon with Tyr-448 in sticks. Catalytic aspartic acids are shown in pink. (D) BVDV RdRp is shown in light blue ribbon (in the same orientation as the *Flavivirus* RdRps in (A)) with a GTP in site *i* – 1 in cyan sticks. The priming loop is represented in blue with Tyr-581 in sticks. Catalytic aspartic acids are represented in pink. (For interpretation of the references to color in this figure legend, the reader is referred to the web version of the article.)

fingers subdomain, explaining the observed loss of activity. The first fingertip which connects to the thumb bears the bNLS (see below) and the other bears motif F. The role of motif F (Bruenn, 2003) is to provide a binding site for incoming NTPs via basic residues. However, the fingertip loop comprising motif F is partially disordered even in the structures of active *Flavivirus* RdRps. Surprisingly, the ordered part runs perpendicular to motif F in other RdRps and is composed of an α-helix rather than a β-strand (Fig. 4). Thus, motif F is not localized in the upper part of the NTP tunnel as in other RdRps and cannot provide a binding site for incoming NTPs. An important conformational change should occur before the initiation of polymerization to allow the structural elements bearing motif F to take their proper position for catalysis.

Another interesting feature of the fingers subdomain of *Flavivirus* RdRps is the presence of a loop, which protrudes towards the active site. In other RdRps, the corresponding loop has a distinct conformation and is located at the entrance of the RNA template-binding groove, establishing contact with the template. It corresponds to motif G in primer-dependent RdRps (Gorbalenya et al., 2002; Ferrer-Orta et al., 2004), and we will therefore call it the G-loop. Its tip is partially disordered in the *Flavivirus* RdRp structures, suggesting conformational flexibility (Fig. 4). Its location near the active site coincides with the position of the C termini in HCV and BVDV RdRps. In analogy to the HCV RdRp C terminus which has been shown to regulate the RdRp activity by preventing binding of both RNA and incoming NTPs (Adachi et al., 2002; Leveque et al., 2003), the *Flavivirus* G-loop could play a similar role.

In summary, the fingers subdomain is highly mobile and concerted conformational changes are likely to occur upon initiation, involving in particular motif F and the G-loop. Thus, we propose that *Flavivirus* RdRps have been captured in a conformation, which corresponds to a pre-initiation mode. Interestingly, both structures show this particular conformation although they crystallized in different space groups. Subsequently, conformational changes in the fingers subdomain may be transmitted to the thumb via the fingertips, which connect the two subdomains in the initiation stage, leading to a more global conformational change of the RdRp structure (see below).

4.5. The thumb subdomain

The interface between the palm and the C-terminal thumb subdomain corresponds to two anti-parallel β-strands and constitutes motif E (Fig. 4), which has been shown to play a role in the binding of the priming NTP. The rest of the thumb is made of eight α-helices with a different topology compared to HCV and BVDV RdRps. In contrast to HCV, BVDV and Norwalk virus RdRps (Adachi et al., 2002; Choi et al., 2004; Ng et al., 2004), the C terminus of the RdRp is not expected to access the active site and play a regulatory role. A greater than 40 Å distance between the active site and the last visible C-terminal residue, Leu-899, of the WNV RdRp structure precludes a role in the regulation of *Flavivirus* RNA synthesis.

The most interesting feature of the thumb subdomain is the presence of a loop protruding from the thumb towards the active site (Figs. 4 and 5A). This putative priming loop is a characteristic feature of *de novo* polymerases (Ferrer-Orta et al., 2006). Such loops have been shown to play an essential role in *de novo* RNA polymerization by phi6 and HCV RdRps (Hong et al., 2001; Laurila et al., 2002; van Dijk et al., 2004). The conformation of the priming loops of DENV3 and WNV RdRps is unique, bearing no obvious secondary structure. It comprises residues 792–804 in DENV3 RdRp (corresponding to 796–809 in WNV RdRp). In other *de novo* RdRps, aromatic residues (Tyr-630 in phi6, Tyr-448 in HCV, Tyr-581 in BVDV RdRps) in the priming loops have been proposed to promote stabilization of the *de novo* initiation complex. Indeed, a stabilizing stacking interaction of Tyr-630 with the base of the priming NTP has been shown in the *de novo* initiation complex of phi6 RdRp (Butcher et al., 2001). No equivalent tyrosine exists in the priming loop of *Flavivirus* RdRps but residues Trp-795 or His-798 of DENV3 RdRp (Trp-800, His-803 in WNV RdRp), which are conserved in NS5 of all flaviviruses, could play a similar role (see below).

4.6. A model for the initiation complex and 3′dGTP binding site

In *Flavivirus* RdRp, the components of a putative *de novo* initiation complex can be defined as follows: (i) the template RNA whose 3′ end consists of nucleotides CU for both positive and negative strands, (ii) the complementary NTPs to be incorporated, ATP and GTP, (iii) magnesium or manganese ions and (iv) the RdRp. Based on this and the existing *de novo* initiation complex structure of phi6 RdRp (Butcher et al., 2001), we generated a model of the WNV RdRp initiation complex (Fig. 5B). The position of the RNA template and the catalytic ions were thus inferred from the phi6 initiation complex. ATP and GTP were positioned at sites *i* (priming site also named site P) and *i* + 1 (catalytic site C), respectively, described in the phi6 complex and also in HCV RdRp in complex with NTPs (Bressanelli et al., 2002). Most of the residues in sites *i* and *i* + 1 are conserved in DENV3 and WNV RdRps compared to HCV RdRp (Asp-533, Asp-663, Asp-664, Ser-710, Arg-729, Arg-737 in DENV3 RdRp). The final model shows that WNV RdRp in the captured conformation can form a *de novo* initiation complex that is in line with the *de novo* complex structure of phi6 RdRp. Additionally, residue Trp-800 of WNV RdRp was better positioned than His-803 to stack the adenine base of the initiating nucleotide and was thus proposed to serve as an initiation platform of *Flavivirus* RdRp.

Soaking of DENV3 RdRp crystals in 3′dGTP resulted in a bound triphosphate moiety (tP) coordinated by Ser-710, Arg-729 and Arg-737 (Fig. 5A). Mutations of corresponding residues in BVDV and HCV RdRps have shown that they were involved in *de novo* initiation (Lai et al., 1999; Ranjith-Kumar et al., 2003). The orientation of the tP moiety is consistent with a stacking interaction between the GTP base and the residue Trp-795 of the priming loop. It corresponds to WNV RdRp residue Trp-800 and thus validates at least in part our initiation complex model (see above). The 3′dGTP is positioned at about 7 Å from the active site between a tP moiety of a UTP attributed to the *i* site (Fig. 5C) in a HCV RdRp complex (Bressanelli et al., 2002) and a tP of a GTP attributed to a so-called *i* – 1 site (Fig. 5D) present in a BVDV RdRp complex (Choi et al., 2004). The *i* – 1 binding site is located between the priming loop and the *i* site. For BVDV RdRp, it was proposed that the bound GTP stacking the Tyr residue in the initiation loop acts itself as an initiation platform by stacking the priming NTP (Choi et al., 2004). The existence of GTP binding to the *i* – 1 site was also proposed for the RdRp of *Flaviviridae* member GBV-C based on modeling studies (Ferron et al., 2005). A special role for GTP, and thus a putative indication of a GTP *i* – 1 site, has also been observed in biochemical experiments. Firstly, an unusual high concentration of GTP is required for *de novo* initiation (Nomaguchi et al., 2003). Secondly, a preference by DENV2 and WNV RdRp was observed for *de novo* initiation on homopolymeric template poly(rC) (thus using GTP) in comparison to poly(rU) or poly(rA) (Selisko et al., 2006). Thirdly, there are indications for a second GTP binding site on *Flavivirus* RdRps (Selisko et al., 2006). However, additional experiments are necessary to verify the presence of a GTP in the putative *i* – 1 site and clarify its role in RNA synthesis.

A pocket which could correspond to the *i* – 1 binding site exists in DENV-3 RdRp. It is, however, absent in WNV RdRp due to a closer conformation of the priming loop which fills the pocket (Fig. 5A). The different position of the priming loop in WNV RdRp compared to DENV3 RdRp also implies that the 3′dGTP could not

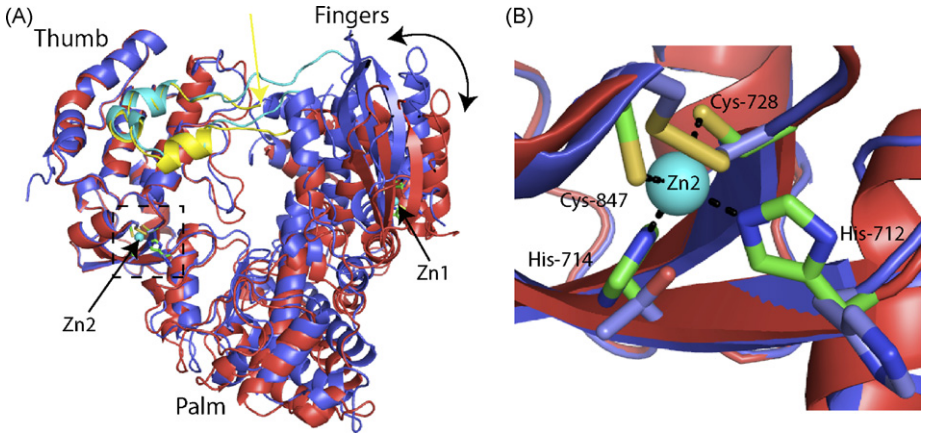

Fig. 6. Structural differences between DENV3 and WNV RdRp and position of zinc ions. "Back" view of DENV3 (in red) and WNV (in blue) RdRps in ribbon representation. (A) The superposition of the thumb subdomains shows a 8° rotation of the fingers subdomain compared to the thumb subdomains. The hinge between the thumb and the rest of the structure is located near the zinc-binding site of the thumb (Zn2). Zinc ions are represented by cyan spheres. Coordinating residues in DENV3 RdRp are shown in green. The finger that maintains the connection between the fingers and thumb subdomains is represented in yellow for DENV3 RdRp and cyan for WNV RdRp. The DENV3 finger is partially disordered; a yellow arrow indicates the interruption. (B) Close-up of Zn2 binding site in DENV3 RdRp. The zinc ion and coordinating residues are represented as in (A). Equivalent residues in WNV RdRp are shown in blue. On the right the difference of the conformation of the proposed hinge histidine 712 between DENV3 and WNV RdRps is shown. A disulfide bond is present in WNV RdRp and the zinc ion is absent. (For interpretation of the references to color in this figure legend, the reader is referred to the web version of the article.)

be positioned in WNV RdRp in the same location as in DENV3 RdRp without a steric clash between triphosphate of the 3′dGTP and the WNV priming loop. This could illustrate a difference between the WNV and DENV3 RdRp initiation mechanism or indicates a necessary movement of WNV RdRp priming loop for initiation.

4.7. Zinc ions

Unexpectedly, zinc ions are present in the structures of DENV3 and WNV RdRp although no zinc was added during purification and crystallization. One zinc-binding site is located in the fingers, another in the thumb subdomain (Zn1 and Zn2, respectively, Fig. 6A). Both are buried within the protein and engage into a tetrahedral coordination. Zn1 is coordinated by DENV3 residues Cys-446, Cys-449, His-441 and the carboxylate group of Glu-437. Interestingly, whereas Zn1 is present in all structures, Zn2 is absent in the active WNV RdRp domain but present in DENV3 RdRp and in the short, inactive form of WNV RdRp. It is coordinated in DENV3 RdRp by His-712, His-714, Cys-728 and Cys-847 (Fig. 6B). A similar coordination exists in the short, inactive form of WNV RdRp even if the residue His-714 is not conserved and is replaced by a threonine. In the catalytically active form of WNV RdRp, the His side chain corresponding to His-712 is pointing in a different direction. Additionally, a disulfide bond is formed between the Cys residues corresponding to Cys-728 and Cys-847 (Fig. 6B). Interestingly, the binding site of Zn2 is located in the vicinity of Ser-710 and Arg-729 which are involved in binding 3′dGTP (see Section 4.6) and correspond to HCV RdRp residues involved in *de novo* initiation and binding to the NTP in the *i* site (Bressanelli et al., 2002).

The position of the Zn2-binding site, in particular His-712, seems to correspond to a hinge between the thumb and the palm subdomain. This hinge supports an 8°-rotation of the thumb subdomain away from the palm subdomain and consequently, and more dramatically, from the finger subdomain. This is best shown by a superposition of the thumb subdomains of DENV3 and WNV RdRps as in Fig. 6A, illustrating the more open global conformation of DENV3 RdRp. The finger whose tip still maintains the connection to the thumb domain in DENV3 RdRp is thus more stretched and partially disordered. A slight rotation (between 1° and 2°) in the same sense also exists between the long and the short form of WNV RdRp. It is tempting to speculate that the global conformational change upon the transition from initiation to elongation includes a subdomain rotation as observed between DENV3 and the short and long form of WNV RdRp and that Zn2 might play a role in its regulation. The more closed WNV RdRp structure needs a wider aperture movement upon the transition to elongation mode what could explain why the transition from initiation to elongation seems to be kinetically more limiting for WNV RdRp compared to DENV RdRp (Fig. 3B; Selisko et al., 2006). Inhibitors which prevent this global change by "freezing" the RdRp in one of these conformations will help understanding of the whole process and may act as efficient antivirals.

4.8. The interaction of the RdRp domain with the MTase domain

The crystal structure of the *Flavivirus* NS5 MTase domain (DENV2) was determined long before that of the RdRp domain (Egloff et al., 2002). Since then several other MTase domains have followed (see Chapter NS5 MTase in this issue). The relative orientation of the two domains in full-length NS5 is still unknown. A model of full-length WNV NS5 is shown in Fig. 7 (Malet et al., 2007). It is based on reverse genetic experiments using a DENV2 infectious clone, the structure of WNV RdRp and a homology model of WNV MTase generated from the DENV2 MTase structure. The central point of the model is the hypothesis that DENV2 MTase domain residues Lys-46, Arg-47 and Glu-49 form part of an interface involving residue Leu512 of the RdRp domain. The triple mutant of the MTase domain failed to produce a significant titer of infectious virus in transfected cells. However, virus could be recovered which contained an additional compensatory mutation Leu512Val in the RdRp domain. As these residues are surface exposed and away from the respective active sites, a model was proposed in which the residues interact directly. A spatial restraint imposed during model building was the proximity of MTase C-terminus at residue 264 and N-terminus of the RdRp domain structure at residue 278 (Fig. 7). Interestingly, in the final model the RNA-substrate binding groove of the MTase domain is positioned near the RdRp ds RNA exit tun-

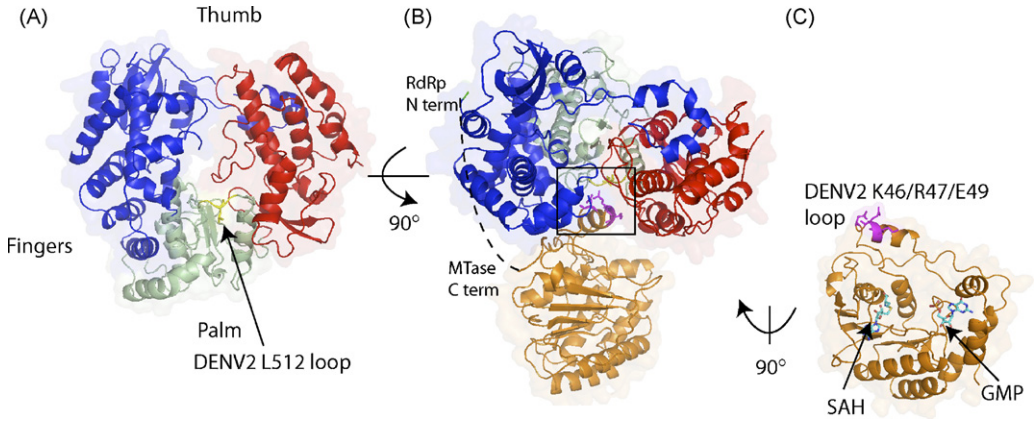

Fig. 7. Model of full-length protein WNV NS5. (A) RdRp subdomains are represented in the same colors as in Fig. 3. The L512-loop is shown in yellow. (B) Model of full-length NS5 with the RdRp rotated by 90° compared to (A). The MTase is presented in orange. The location of the interface of the RdRp L512-loop (in yellow) and the MTase K46/R47/E49-loop (in magenta) is contoured by a black rectangle. A dotted line represents the missing residues between the C-terminal of the MTase and the N-terminal of the RdRp. (C) A 90° rotation of the MTase domain showing the position of the K46/R47/E49-loop (in magenta) away from the active site located between the binding sites of the co-product S-adenosyl-homocysteine (SAH) and the GMP corresponding to the extremity of capped RNA during 2′O-methylation of the first nucleotide A (Egloff et al., 2007). (For interpretation of the references to color in this figure legend, the reader is referred to the web version of the article.)

nel, consistent with RNA cap methylation of the nascent genome occurring after the (+) strand product leaves the RdRp domain.

4.9. The interaction of the Flavivirus RdRp domain with NS3 and importins

The *Flavivirus* proteins NS3 and NS5 have been shown to interact using co-immunoprecipitation experiments (Kapoor et al., 1995). Later, it has been shown that residues 320–368 of DENV2 RdRp interact with the C-terminal domain of NS3 (Johansson et al., 2001). These residues are localized at the "back" of the RdRp including one of the fingertips connecting the fingers and thumb subdomains (see Figs. 4 and 8A). This putative positioning of NS3 close to the entrance of the RNA template is consistent with its helicase activity unwinding ds RNA or RNA secondary structure prior to polymerization. More precise mapping of the interaction zone might give rise to the rational development of inhibitors that impede this essential interaction in the *Flavivirus* replicative complex (see below).

During infection, a proportion of DENV2 and YFV NS5 proteins enter the nucleus (Buckley et al., 1992; Kapoor et al., 1995; Pryor et al., 2007) in contrast to WNV NS5, which shows cytoplasmic and periplasmic localization (Mackenzie et al., 2007; Malet et al., 2007). The transfer of DENV NS5 to the nucleus was proposed to rely on a nuclear import pathway based on the identification of functional NLSs in NS5 and their interaction with the intracellular transport proteins importin α and β (Johansson et al., 2001; Brooks et al., 2002). A high affinity interaction was detected between DENV2 NS5 and importin-α/β heterodimer (27 nM) whereas importin-α and importin-β both bind NS5 with a lower affinity (234 and 510 nM) (Pryor et al., 2007). Therefore, importin-α/β heterodimer is likely to be the nuclear import receptor for NS5. The two NLSs in DENV2 NS5 comprise residues 320–368 (bNLS—interaction with importin-β) and residues 369–389 (a/bNLS—interaction with the α/β importin). The structures of *Flavivirus* RdRp domains have shown that the NLSs form an integral part of the RdRp domain (Fig. 8A and B). Interestingly, the bNLS coincides with the NS3 binding site (Johansson et al., 2001). It consists of two parts: (i) a long helix–turn–helix loop protruding from the fingers domain and interacting with the thumb domain, thus forming part of the fingertip region and (ii) a C-terminal portion that packs at the interface between the back of the finger domain and the palm and

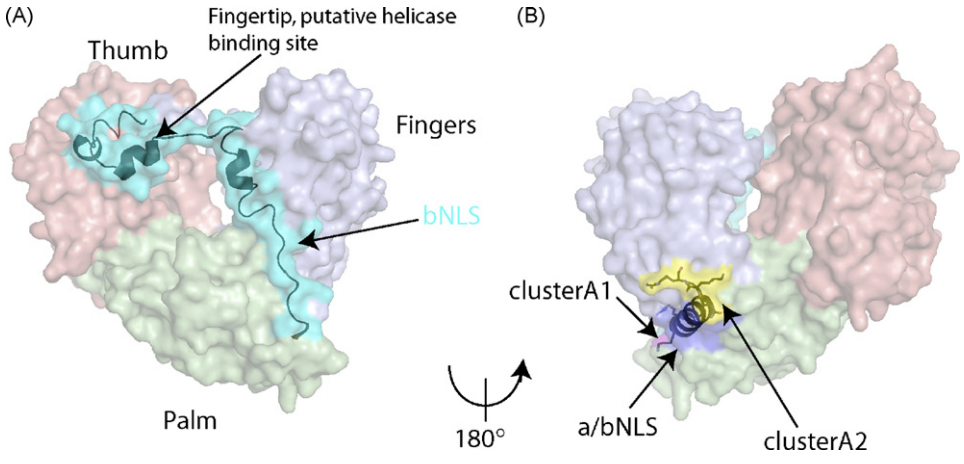

Fig. 8. Position of putative b and a/bNLS on DENV3 RdRp. (A) "Back" view of DENV-3 RdRp in surface representation with subdomains palm, fingers and thumb colored in light green, light blue and light red, respectively. The putative NS3-binding region and the bLNS coincide and are colored in cyan. The secondary structure elements are represented in ribbon. (B) "Front" view of DENV3 RdRp rotated by 180° compared to (A). The a/bNLS helix is colored in blue and represented in ribbon. Residues corresponding to DENV2 basic clusters A1 and A2, necessary for the nuclear import, are shown in magenta and yellow sticks, respectively. (For interpretation of the references to color in this figure legend, the reader is referred to the web version of the article.)

which is made of an α-helix (aa 350–358) parallel to the fingers β-sheet, followed by an extended region (aa 360–368) (Fig. 8A). The putative bipartite a/bNLS of *Flavivirus* RdRps consist of an α-helix which forms the interface between the bottom of the finger domain and the palm (Fig. 8B). We can expect that the overall localization and secondary structure elements of the NLSs present in WNV and DENV3 RdRp are conserved in DENV2 and YFV RdRps, which enter the nucleus. The NLSs are composed of clusters of basic amino acids. For DENV2 RdRp, two cluster of basic residues in the a/bNLS, containing residues Lys-371, Lys-372 for cluster-A1 and Lys387, Lys-388, Lys-389 for cluster-A2 (shown on DENV3 RdRp Fig. 8B) have been shown to be important for efficient nuclear import (Pryor et al., 2007). In DENV3 RdRp not all basic residues of these clusters are conserved and it is not yet known if DENV3 NS5 goes to the nucleus. An equivalent structural scaffold can be found in both BVDV (aa 132–200) and HCV (aa 20–76) RdRps, with a well-conserved overall shape and secondary structure, but no conservation of charged clusters. No functional NLSs have been described in hepaci- or pestiviruses. Thus, subtle differences in NLS geometry and charge distribution may be responsible for distinct behavior towards nuclear import in closely related viruses. The role of the nuclear import of DENV2 NS5 in the viral life cycle is still unclear but putatively important for virus production (Pryor et al., 2007) representing therefore a potential target for drug development.

5. Drug discovery efforts targeted at *Flavivirus* RdRp and replication

Antiviral drugs targeting the RdRp may either directly inhibit polymerase activity or essential interactions either with other proteins (within or outside the replicative complex) or with the RNA template or promoter elements.

In general, polymerase activity inhibitors can be assigned to two broad categories on the basis of their chemical structure and mechanism of action: nucleoside analogue inhibitors (NI) and non-nucleoside analogue inhibitors (NNI). Nucleoside analogues are generally converted to nucleotide analogues by host cell kinases. NIs target the active site of the polymerase. They can either compete with natural NTP substrates or/and act as 'chain terminators' (De Francesco and Carfi, 2007), or cause of a mutational 'error catastrophe' by being incorporated into the elongating nascent RNA molecule (Crotty et al., 2001; Pfeiffer and Kirkegaard, 2003). NIs have been discovered through the rational search of substrate analogues, and they often possess a broad-spectrum antiviral activity. Few molecules have been reported so far as *Flavivirus* RdRp NIs. GTP analogs 3′dGTP, ddGTP, 3′-dioxolane 3′dGTP, and 2′-O-methyl-GTP showed low micromolar IC_{50} values in *in vitro* DENV2 RdRp activity tests using a poly(rC) template (Romette et al., 2005; Yap et al., 2007). The second category of compounds, NNIs, bind mainly to allosteric surface cavities of the target polymerase. They might cause a conformational change that renders the polymerase inactive, or trap it in a functional conformation but impeding an essential conformational transition between initiation and elongation. Allosteric inhibition has been shown to be a highly effective strategy suppressing HCV RdRp and HIV reverse transcriptase activity (De Clercq, 2005). There is one report on a putative NNI, ammonium-21-tungsto-9-antimonate also named HPA 23, of DENV2 RdRp (Bartholomeusz et al., 1994). This NNI, also shown to inhibit HIV reverse transcriptase, was proposed to compete with the nucleic acid template (Herve et al., 1983), thus it is not an allosteric inhibitor. Altogether, there are many examples of viral polymerase inhibitors, both NIs and NNIs, used in the clinic, many of them targeting the HIV reverse transcriptase (De Clercq, 2005). Several inhibitors of HCV RdRp are currently undergoing clinical trials (De Francesco and Carfi, 2007).

Inhibitors of protein–protein or protein–RNA interactions involving viral polymerases are less explored as antiviral drugs. Effective antiviral molecules that seem to inhibit interactions of the viral polymerase within the replicative complex have been reported, e.g. for herpes virus (Pilger et al., 2004) and pestiviruses (Paeshuyse et al., 2006; Paeshuyse et al., 2007). The search for antivirals against *Flavivirus* RdRps and RNA replication can be considered to be in its initial phase and *Flavivirus* RdRp crystal structures will undoubtedly help the whole process.

5.1. Potential ligand binding sites

The knowledge of *Flavivirus* RdRp structures allows performing a surface shape analysis with the aim to predict cavities that could potentially correspond to allosteric inhibitor binding sites. We used the programs PASS (Brady and Stouten, 2000) and CastP (Dundas et al., 2006) and selected cavities identified by both programs and having the largest volume based on Connolly's molecular surface. Cavities were not selected when they were too close to disordered regions and corresponded to the whole active site cavity. As positive control, both programs were applied with the same criteria using HCV RdRp. Eight cavities were found. Three of them correspond to already identified allosteric inhibitor binding sites of HCV RdRp (De Francesco and Carfi, 2007). In DENV3 and WNV RdRp two and five cavities were found, respectively (shown in Fig. 9A and B on WNV RdRp). The two cavities (named cavity A and B) identified in both RdRps are located in the thumb subdomain. Cavity A is the largest with a volume of 169 $Å^3$. Residues which form that cavity are listed in Fig. 9C. In particular, Tyr-867 forms the upper part of the cavity and could promote a stacking interaction with a ligand containing an aromatic ring. Residues 810–814 (main chain atoms), which constitute the end of the priming loop, form the lower part of the cavity. Binding of a compound in that cavity could thus potentially impair the conformational change of the priming loop necessary for the transition to elongation. Cavity B is located on top of the thumb and has a volume of 77 $Å^3$. Main residues lining this cavity are listed in Fig. 9C. Three additional cavities are present only in WNV RdRp, located in the thumb (cavity C and D) and in the fingers subdomain (cavity E). All the predicted cavities are completely different from the established inhibitor-binding sites of HCV RdRp. The size and the shape of the predicted cavities are compatible with the binding of small-molecule inhibitors in potential allosteric sites, they could thus represent "druggable pockets". Especially cavity A and B predicted for both DENV3 and WNV RdRp might be used as a starting point for structure-based drug design a first possible approach being virtual screening. Inhibition, mutational and structural studies are ongoing to determine if they are indeed allosteric inhibitor-binding sites.

5.2. In vitro enzymatic screening of Flavivirus polymerase inhibitors

The RdRp activity of DENV2 or WNV NS5 was not affected by the presence of the MTase domain (see above). Thus, a radioactive assay of the DENV2 RdRp domain on homopolymeric template poly(rC) (Selisko et al., 2006) has been adapted in our group to high-throughput screening (HTS) format for the screening of several academic and commercial chemical libraries containing potential NNIs of a large structural diversity. In another approach headed by the Novartis Institute of Tropical Diseases Singapore (NITD), a scintillation proximity assay using DENV2 full-length NS5 (Yap et al., 2007) allowed HTS of more than a million compounds. Both HTS gave rise to various hits (unpublished results), which are studied

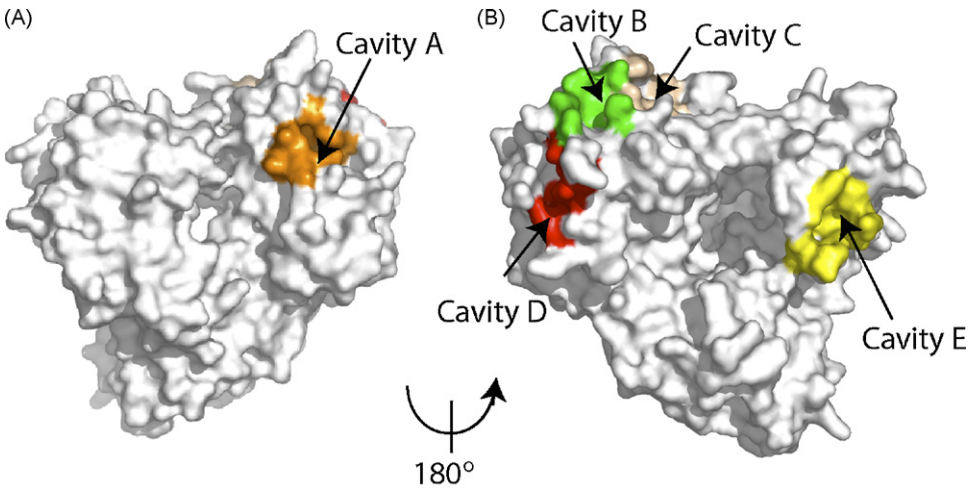

(C)

CavityA	K756, Q760, S763, N777, C780, V785, T806, E807, D808, M809, L810, Y882
CavityB	L326, L327, K329, T858, W859, N862, I863, A866

Fig. 9. Position of cavities and putative allosteric sites on WNV RdRp. WNV RdRp cavities found by both programs, Pass and CastP, are represented in color on the surface and are named by letters. Cavities A and B were also found on DENV3 RdRp. (A) "Front" view showing cavity A. (B) "Back" view showing cavities B, C and D. (C) DENV3 residues constituting the putative allosteric sites A and B are given.

regarding their mechanism of action, their binding sites, and their potency in a cellular context. Structure activity relationship studies of this hit-to-lead process are on going.

5.3. Inhibition of the interaction between the polymerase and its partners

Novel antiviral strategies targeting the RdRp of flaviviruses might also be developed based on the prevention of its interactions with other proteins that are essential for the virus life cycle. One example is the interaction between the RdRp domain of NS5 and the helicase domain of NS3 of DENV2. A colony lift assay was set up using a yeast two-hybrid system in which the NS5–NS3 interaction activates transcription of the reporter gene lacZ. The resultant β-galactosidase activity indicates the binding strength. This assay in a 96-well plate format allows testing compounds in a high-throughput manner (Vasudevan et al., 2001).

5.4. Cell-based screening of flavivirus polymerase inhibitors

Besides classic virus infection, infectious RNA clones and subgenomic RNA replicons containing only the non-structural replicative proteins have been set up as useful tools in HTS of potential inhibitory compounds. Such *in vivo* cell-based assays present the advantage of being carried out in the context of the full replication complex, including viral and cellular proteins. Screening of libraries of small molecules using a luciferase-expressing WNV subgenomic-replicon system allowed the identification of several class of compounds (parazolotrahydrothophenes, pyrozolopyrimidines, pyrazolines, xanthanes, acridines, quinolines, sulfonamides) that reduced luciferase and WNV viral protein accumulation as well as viral RNA copy number in the replicon-containing cells (Goodell et al., 2006; Gu et al., 2006; Puig-Basagoiti et al., 2006; Noueiry et al., 2007). Some of these compounds have been shown to inhibit the replication of DENV or other flaviviruses (Goodell et al., 2006; Puig-Basagoiti et al., 2006; Noueiry et al., 2007). Recently, the first luciferase expressing DENV2 subgenomic-replicon system has been set up and tested with the broad-spectrum antiviral ribavirin (Ng et al., 2007).

Cell-based assays will identify general inhibitors of virus growth, amongst which are inhibitors of the RdRp. Active compounds need then to be assayed in *in vitro* RdRp assays. Alternatively or in parallel, if resistant viruses or replicons can be selected, their nucleotide sequence may point to the target of the compound.

6. Conclusion

We are witnessing an increasing incidence and impact of outbreaks caused by DENV, WNV and other flaviviruses. Thanks to many academic and corporate research efforts in the world, drug design against flaviviruses is also robustly emerging. Drug design against the *Flavivirus* polymerase has recently switched gear mainly due to important advances in its enzymatic and structural characterization. With the ongoing characterization of other *Flavivirus* targets – such as the protease, helicase, and methyltransferase – paving the way for combined therapies, anti-*Flavivirus* drug prospectives are increasingly bright.

Acknowledgements

This work was supported in part by the VIZIER integrated project (LSHG-CT-2004-511960) of the European Union 6th Framework, by

the Direction Générale de l'Armement (contrat no. 07co404), and the Agence Nationale de la Recherche (ANR-07-BLAN-0285-01). We thank Xavier de Lamballerie, Ernest Gould, Gérard Bricogne, Alexander Khromykh and Andrew Davidson for helpful discussions and Delphine Benarroch, Marie-Pierre Egloff, Hélène Dutartre, Claire Debarnot, Frédéric Peyrane, Karine Barral, Sylvain Marc, Mohamed Ben Rahou and Marilyne Blémont for their contribution at various stages of the project.

References

Ackermann, M., Padmanabhan, R., 2001. De novo synthesis of RNA by the dengue virus RNA-dependent RNA polymerase exhibits temperature dependence at the initiation but not elongation phase. J. Biol. Chem. 276, 39926–39937.

Adachi, T., Ago, H., Habuka, N., Okuda, K., Komatsu, M., Ikeda, S., Yatsunami, K., 2002. The essential role of C-terminal residues in regulating the activity of hepatitis C virus RNA-dependent RNA polymerase. Biochim. Biophys. Acta. 1601, 38–48.

Ago, H., Adachi, T., Yoshida, A., Yamamoto, M., Habuka, N., Yatsunami, K., Miyano, M., 1999. Crystal structure of the RNA-dependent RNA polymerase of hepatitis C virus. Structure 7, 1417–1426.

Alvarez, D.E., Lodeiro, M.F., Luduena, S.J., Pietrasanta, L.I., Gamarnik, A.V., 2005. Long-range RNA–RNA interactions circularize the dengue virus genome. J. Virol. 79, 6631–6643.

Bartholomeusz, A., Tomlinson, E., Wright, P.J., Birch, C., Locarnini, S., Weigold, H., Marcuccio, S., Holan, G., 1994. Use of a flavivirus RNA-dependent RNA polymerase assay to investigate the antiviral activity of selected compounds. Antiviral Res. 24, 341–350.

Bartholomeusz, A.I., Wright, P.J., 1993. Synthesis of dengue virus RNA in vitro: initiation and the involvement of proteins NS3 and NS5. Arch. Virol. 128, 111–121.

Brady Jr., G.P., Stouten, P.F., 2000. Fast prediction and visualization of protein binding pockets with PASS. J. Comput. Aided Mol. Des. 14, 383–401.

Bressanelli, S., Tomei, L., Rey, F.A., De Francesco, R., 2002. Structural analysis of the hepatitis C virus RNA polymerase in complex with ribonucleotides. J. Virol. 76, 3482–3492.

Bressanelli, S., Tomei, L., Roussel, A., Incitti, I., Vitale, R.L., Mathieu, M., De Francesco, R., Rey, F.A., 1999. Crystal structure of the RNA-dependent RNA polymerase of hepatitis C virus. Proc. Natl. Acad. Sci. U.S.A. 96, 13034–13039.

Brooks, A.J., Johansson, M., John, A.V., Xu, Y., Jans, D.A., Vasudevan, S.G., 2002. The interdomain region of dengue NS5 protein that binds to the viral helicase NS3 contains independently functional importin beta 1 and importin alpha/beta-recognized nuclear localization signals. J. Biol. Chem. 277, 36399–36407.

Bruenn, J.A., 1991. Relationships among the positive strand and double-strand RNA viruses as viewed through their RNA-dependent RNA polymerases. Nucleic Acids Res. 19, 217–226.

Bruenn, J.A., 2003. A structural and primary sequence comparison of the viral RNA-dependent RNA polymerases. Nucleic Acids Res. 31, 1821–1829.

Buckley, A., Gaidamovich, S., Turchinskaya, A., Gould, E.A., 1992. Monoclonal antibodies identify the NS5 yellow fever virus non-structural protein in the nuclei of infected cells. J. Gen. Virol. 73 (Pt 5), 1125–1130.

Butcher, S.J., Grimes, J.M., Makeyev, E.V., Bamford, D.H., Stuart, D.I., 2001. A mechanism for initiating RNA-dependent RNA polymerization. Nature 410, 235–240.

Castro, C., Smidansky, E., Maksimchuk, K.R., Arnold, J.J., Korneeva, V.S., Gotte, M., Konigsberg, W., Cameron, C.E., 2007. Two proton transfers in the transition state for nucleotidyl transfer catalyzed by RNA- and DNA-dependent RNA and DNA polymerases. Proc. Natl. Acad. Sci. U.S.A. 104, 4267–4272.

Cerutti, H., Casas-Mollano, J.A., 2006. On the origin and functions of RNA-mediated silencing: from protists to man. Curr. Genet. 50, 81–99.

Chaturvedi, U.C., Shrivastava, R., Nagar, R., 2005. Dengue vaccines: problems and prospects. Indian J. Med. Res. 121, 639–652.

Choi, K.H., Groarke, J.M., Young, D.C., Kuhn, R.J., Smith, J.L., Pevear, D.C., Rossmann, M.G., 2004. The structure of the RNA-dependent RNA polymerase from bovine viral diarrhea virus establishes the role of GTP in de novo initiation. Proc. Natl. Acad. Sci. U.S.A. 101, 4425–4430.

Chu, P.W., Westaway, E.G., 1985. Replication strategy of Kunjin virus: evidence for recycling role of replicative form RNA as template in semiconservative and asymmetric replication. Virology 140, 68–79.

Cleaves, G.R., Ryan, T.E., Schlesinger, R.W., 1981. Identification and characterization of type 2 dengue virus replicative intermediate and replicative form RNAs. Virology 111, 73–83.

Corver, J., Lenches, E., Smith, K., Robison, R.A., Sando, T., Strauss, E.G., Strauss, J.H., 2003. Fine mapping of a cis-acting sequence element in yellow fever virus RNA that is required for RNA replication and cyclization. J. Virol. 77, 2265–2270.

Crotty, S., Cameron, C.E., Andino, R., 2001. RNA virus error catastrophe: direct molecular test by using ribavirin. Proc. Natl. Acad. Sci. U.S.A. 98, 6895–6900.

De Clercq, E., 2005. Recent highlights in the development of new antiviral drugs. Curr. Opin. Microbiol. 8, 552–560.

De Francesco, R., Carfi, A., 2007. Advances in the development of new therapeutic agents targeting the NS3-4A serine protease or the NS5B RNA-dependent RNA polymerase of the hepatitis C virus. Adv. Drug Deliv. Rev. 59, 1242–1262.

Dundas, J., Ouyang, Z., Tseng, J., Binkowski, A., Turpaz, Y., Liang, J., 2006. CASTp: computed atlas of surface topography of proteins with structural and topographical mapping of functionally annotated residues. Nucleic Acids Res. 34, W116–118.

Egloff, M.P., Benarroch, D., Selisko, B., Romette, J.L., Canard, B., 2002. An RNA cap (nucleoside-2′-O-)-methyltransferase in the flavivirus RNA polymerase NS5: crystal structure and functional characterization. EMBO J. 21, 2757–2768.

Egloff, M.P., Decroly, E., Malet, H., Selisko, B., Benarroch, D., Ferron, F., Canard, B., 2007. Structural and functional analysis of methylation and 5′-RNA sequence requirements of short capped RNAs by the methyltransferase domain of dengue virus NS5. J. Mol. Biol. 372, 723–736.

Ferrer-Orta, C., Arias, A., Escarmis, C., Verdaguer, N., 2006. A comparison of viral RNA-dependent RNA polymerases. Curr. Opin. Struct. Biol. 16, 27–34.

Ferrer-Orta, C., Arias, A., Perez-Luque, R., Escarmis, C., Domingo, E., Verdaguer, N., 2004. Structure of foot-and-mouth disease virus RNA-dependent RNA polymerase and its complex with a template-primer RNA. J. Biol. Chem. 279, 47212–47221.

Ferrer-Orta, C., Arias, A., Perez-Luque, R., Escarmis, C., Domingo, E., Verdaguer, N., 2007. Sequential structures provide insights into the fidelity of RNA replication. Proc. Natl. Acad. Sci. U.S.A. 104, 9463–9468.

Ferron, F., Bussetta, C., Dutartre, H., Canard, B., 2005. The modeled structure of the RNA dependent RNA polymerase of GBV-C Virus suggests a role for motif E in Flaviviridae RNA polymerases. BMC Bioinform. 6, 255.

Filomatori, C.V., Lodeiro, M.F., Alvarez, D.E., Samsa, M.M., Pietrasanta, L., Gamarnik, A.V., 2006. A 5′ RNA element promotes dengue virus RNA synthesis on a circular genome. Genes Dev. 20, 2238–2249.

Goodell, J.R., Puig-Basagoiti, F., Forshey, B.M., Shi, P.Y., Ferguson, D.M., 2006. Identification of compounds with anti-West Nile Virus activity. J. Med. Chem. 49, 2127–2137.

Gorbalenya, A.E., Pringle, F.M., Zeddam, J.L., Luke, B.T., Cameron, C.E., Kalmakoff, J., Hanzlik, T.N., Gordon, K.H., Ward, V.K., 2002. The palm subdomain-based active site is internally permuted in viral RNA-dependent RNA polymerases of an ancient lineage. J. Mol. Biol. 324, 47–62.

Gu, B., Ouzunov, S., Wang, L., Mason, P., Bourne, N., Cuconati, A., Block, T.M., 2006. Discovery of small molecule inhibitors of West Nile virus using a high-throughput sub-genomic replicon screen. Antiviral Res. 70, 39–50.

Guyatt, K.J., Westaway, E.G., Khromykh, A.A., 2001. Expression and purification of enzymatically active recombinant RNA-dependent RNA polymerase (NS5) of the flavivirus Kunjin. J. Virol. Methods 92, 37–44.

Herve, M., Sinoussi-Barre, F., Chermann, J.C., Herve, G., Jasmin, C., 1983. Correlation between structure of polyoxotungstates and their inhibitory activity on polymerases. Biochem. Biophys. Res. Commun. 116, 222–229.

Hong, Z., Cameron, C.E., Walker, M.P., Castro, C., Yao, N., Lau, J.Y., Zhong, W., 2001. A novel mechanism to ensure terminal initiation by hepatitis C virus NS5B polymerase. Virology 285, 6–11.

Huang, H., Chopra, R., Verdine, G.L., Harrison, S.C., 1998. Structure of a covalently trapped catalytic complex of HIV-1 reverse transcriptase: implications for drug resistance. Science 282, 1669–1675.

Johansson, M., Brooks, A.J., Jans, D.A., Vasudevan, S.G., 2001. A small region of the dengue virus-encoded RNA-dependent RNA polymerase, NS5, confers interaction with both the nuclear transport receptor importin-beta and the viral helicase NS3. J. Gen. Virol. 82, 735–745.

Kao, C.C., Del Vecchio, A.M., Zhong, W., 1999. De novo initiation of RNA synthesis by a recombinant flaviviridae RNA-dependent RNA polymerase. Virology 253, 1–7.

Kapoor, M., Zhang, L., Ramachandra, M., Kusukawa, J., Ebner, K.E., Padmanabhan, R., 1995. Association between NS3 and NS5 proteins of dengue virus type 2 in the putative RNA replicase is linked to differential phosphorylation of NS5. J. Biol. Chem. 270, 19100–19106.

Khromykh, A.A., Meka, H., Guyatt, K.J., Westaway, E.G., 2001. Essential role of cyclization sequences in flavivirus RNA replication. J. Virol. 75, 6719–6728.

Koonin, E.V., 1991. The phylogeny of RNA-dependent RNA polymerases of positive-strand RNA viruses. J. Gen. Virol. 72 (Pt 9), 2197–2206.

Lai, V.C., Kao, C.C., Ferrari, E., Park, J., Uss, A.S., Wright-Minogue, J., Hong, Z., Lau, J.Y., 1999. Mutational analysis of bovine viral diarrhea virus RNA-dependent RNA polymerase. J. Virol. 73, 10129–10136.

Laurila, M.R., Makeyev, E.V., Bamford, D.H., 2002. Bacteriophage phi 6 RNA-dependent RNA polymerase: molecular details of initiating nucleic acid synthesis without primer. J. Biol. Chem. 277, 17117–17124.

Lesburg, C.A., Cable, M.B., Ferrari, E., Hong, Z., Mannarino, A.F., Weber, P.C., 1999. Crystal structure of the RNA-dependent RNA polymerase from hepatitis C virus reveals a fully encircled active site. Nat. Struct. Biol. 6, 937–943.

Leveque, V.J., Johnson, R.B., Parsons, S., Ren, J., Xie, C., Zhang, F., Wang, Q.M., 2003. Identification of a C-terminal regulatory motif in hepatitis C virus RNA-dependent RNA polymerase: structural and biochemical analysis. J. Virol. 77, 9020–9028.

Lo, M.K., Tilgner, M., Bernard, K.A., Shi, P.Y., 2003. Functional analysis of mosquito-borne flavivirus conserved sequence elements within 3′ untranslated region of West Nile virus by use of a reporting replicon that differentiates between viral translation and RNA replication. J. Virol. 77, 10004–10014.

Luo, G., Hamatake, R.K., Mathis, D.M., Racela, J., Rigat, K.L., Lemm, J., Colonno, R.J., 2000. De novo initiation of RNA synthesis by the RNA-dependent RNA polymerase (NS5B) of hepatitis C virus. J. Virol. 74, 851–863.

Mackenzie, J.M., Kenney, M.T., Westaway, E.G., 2007. West Nile virus strain Kunjin NS5 polymerase is a phosphoprotein localized at the cytoplasmic site of viral RNA synthesis. J. Gen. Virol. 88, 1163–1168.

Mackenzie, J.S., Gubler, D.J., Petersen, L.R., 2004. Emerging flaviviruses: the spread and resurgence of Japanese encephalitis West Nile and dengue viruses. Nat. Med. 10, S98–109.

Malet, H., Egloff, M.P., Selisko, B., Butcher, R.E., Wright, P.J., Roberts, M., Gruez, A., Sulzenbacher, G., Vonrhein, C., Bricogne, G., Mackenzie, J.M., Khromykh, A.A., Davidson, A.D., Canard, B., 2007. Crystal structure of the RNA polymerase domain of the West Nile virus non-structural protein 5. J. Biol. Chem. 282, 10678–10689.

Mandl, C.W., Kunz, C., Heinz, F.X., 1991. Presence of poly(A) in a flavivirus: significant differences between the 3′ noncoding regions of the genomic RNAs of tick-borne encephalitis virus strains. J. Virol. 65, 4070–4077.

Ng, C.Y., Gu, F., Phong, W.Y., Chen, Y.L., Lim, S.P., Davidson, A., Vasudevan, S.G., 2007. Construction and characterization of a stable subgenomic dengue virus type 2 replicon system for antiviral compound and siRNA testing. Antiviral Res. 76, 222–231.

Ng, K.K., Pendas-Franco, N., Rojo, J., Boga, J.A., Machin, A., Alonso, J.M., Parra, F., 2004. Crystal structure of norwalk virus polymerase reveals the carboxyl terminus in the active site cleft. J. Biol. Chem. 279, 16638–16645.

Nomaguchi, M., Ackermann, M., Yon, C., You, S., Padmanabhan, R., 2003. De novo synthesis of negative-strand RNA by Dengue virus RNA-dependent RNA polymerase in vitro: nucleotide, primer, and template parameters. J. Virol. 77, 8831–8842.

Nomaguchi, M., Teramoto, T., Yu, L., Markoff, L., Padmanabhan, R., 2004. Requirements for West Nile virus (−)- and (+)-strand subgenomic RNA synthesis in vitro by the viral RNA-dependent RNA polymerase expressed in Escherichia coli. J. Biol. Chem. 279, 12141–12151.

Noueiry, A.O., Olivo, P.D., Slomczynska, U., Zhou, Y., Buscher, B., Geiss, B., Engle, M., Roth, R.M., Chung, K.M., Samuel, M., Diamond, M.S., 2007. Identification of novel small-molecule inhibitors of West Nile virus infection. J. Virol. 81, 11992–12004.

Oh, J.W., Ito, T., Lai, M.M., 1999. A recombinant hepatitis C virus RNA-dependent RNA polymerase capable of copying the full-length viral RNA. J. Virol. 73, 7694–7702.

Paeshuyse, J., Chezal, J.M., Froeyen, M., Leyssen, P., Dutartre, H., Vrancken, R., Canard, B., Letellier, C., Li, T., Mittendorfer, H., Koenen, F., Kerkhofs, P., De Clercq, E., Herdewijn, P., Puerstinger, G., Gueiffier, A., Chavignon, O., Teulade, J.C., Neyts, J., 2007. The imidazopyrrolopyridine analogue AG110 is a novel, highly selective inhibitor of pestiviruses that targets the viral RNA-dependent RNA polymerase at a hot spot for inhibition of viral replication. J. Virol. 81, 11046–11053.

Paeshuyse, J., Leyssen, P., Mabery, E., Boddeker, N., Vrancken, R., Froeyen, M., Ansari, I.H., Dutartre, H., Rozenski, J., Gil, L.H., Letellier, C., Lanford, R., Canard, B., Koenen, F., Kerkhofs, P., Donis, R.O., Herdewijn, P., Watson, J., De Clercq, E., Puerstinger, G., Neyts, J., 2006. A novel, highly selective inhibitor of pestivirus replication that targets the viral RNA-dependent RNA polymerase. J. Virol. 80, 149–160.

Pfeiffer, J.K., Kirkegaard, K., 2003. A single mutation in poliovirus RNA-dependent RNA polymerase confers resistance to mutagenic nucleotide analogs via increased fidelity. Proc. Natl. Acad. Sci. U.S.A. 100, 7289–7294.

Pilger, B.D., Cui, C., Coen, D.M., 2004. Identification of a small molecule that inhibits herpes simplex virus DNA Polymerase subunit interactions and viral replication. Chem. Biol. 11, 647–654.

Poch, O., Sauvaget, I., Delarue, M., Tordo, N., 1989. Identification of four conserved motifs among the RNA-dependent polymerase encoding elements. EMBO J. 8, 3867–3874.

Pryor, M.J., Rawlinson, S.M., Butcher, R.E., Barton, C.L., Waterhouse, T.A., Vasudevan, S.G., Bardin, P.G., Wright, P.J., Jans, D.A., Davidson, A.D., 2007. Nuclear localization of dengue virus nonstructural protein 5 through its importin alpha/beta-recognized nuclear localization sequences is integral to viral infection. Traffic 8, 795–807.

Pugachev, K.V., Guirakhoo, F., Trent, D.W., Monath, T.P., 2003. Traditional and novel approaches to flavivirus vaccines. Int. J. Parasitol. 33, 567–582.

Puig-Basagoiti, F., Tilgner, M., Forshey, B.M., Philpott, S.M., Espina, N.G., Wentworth, D.E., Goebel, S.J., Masters, P.S., Falgout, B., Ren, P., Ferguson, D.M., Shi, P.Y., 2006. Triaryl pyrazoline compound inhibits flavivirus RNA replication. Antimicrob. Agents Chemother. 50, 1320–1329.

Ranjith-Kumar, C.T., Gutshall, L., Sarisky, R.T., Kao, C.C., 2003. Multiple interactions within the hepatitis C virus RNA polymerase repress primer-dependent RNA synthesis. J. Mol. Biol. 330, 675–685.

Ray, D., Shah, A., Tilgner, M., Guo, Y., Zhao, Y., Dong, H., Deas, T.S., Zhou, Y., Li, H., Shi, P.Y., 2006. West Nile virus 5′-cap structure is formed by sequential guanine N-7 and ribose 2′-O methylations by nonstructural protein 5. J. Virol. 80, 8362–8370.

Rice, C.M., Lenches, E.M., Eddy, S.R., Shin, S.J., Sheets, R.L., Strauss, J.H., 1985. Nucleotide sequence of yellow fever virus: implications for flavivirus gene expression and evolution. Science 229, 726–733.

Romette, J., Selisko, B., Egloff, M., Benarroch, D., Canard, B., 2005. Active truncated form of the RNA polymerase of flavivirus. US Patent 10/857244. See website http://www.freepatentsonline.com/y2005/0048472.html.

Selisko, B., Dutartre, H., Guillemot, J.C., Debarnot, C., Benarroch, D., Khromykh, A., Despres, P., Egloff, M.P., Canard, B., 2006. Comparative mechanistic studies of de novo RNA synthesis by flavivirus RNA-dependent RNA polymerases. Virology 351, 145–158.

Steffens, S., Thiel, H.J., Behrens, S.E., 1999. The RNA-dependent RNA polymerases of different members of the family Flaviviridae exhibit similar properties in vitro. J. Gen. Virol. 80 (Pt 10), 2583–2590.

Steitz, T.A., 1998. A mechanism for all polymerases. Nature 391, 231–232.

Tan, B.H., Fu, J., Sugrue, R.J., Yap, E.H., Chan, Y.C., Tan, Y.H., 1996. Recombinant dengue type 1 virus NS5 protein expressed in *Escherichia coli* exhibits RNA-dependent RNA polymerase activity. Virology 216, 317–325.

Tao, Y., Farsetta, D.L., Nibert, M.L., Harrison, S.C., 2002. RNA synthesis in a cage—structural studies of reovirus polymerase lambda3. Cell 111, 733–745.

van Dijk, A.A., Makeyev, E.V., Bamford, D.H., 2004. Initiation of viral RNA-dependent RNA polymerization. J. Gen. Virol. 85, 1077–1093.

Vasudevan, S.G., Johansson, M., Brooks, A.J., Llewellyn, L.E., Jans, D.A., 2001. Characterisation of inter- and intra-molecular interactions of the dengue virus RNA dependent RNA polymerase as potential drug targets. Farmaco 56, 33–36.

Whitehead, S.S., Blaney, J.E., Durbin, A.P., Murphy, B.R., 2007. Prospects for a dengue virus vaccine. Nat. Rev. Microbiol. 5, 518–528.

Yap, T.L., Xu, T., Chen, Y.L., Malet, H., Egloff, M.P., Canard, B., Vasudevan, S.G., Lescar, J., 2007. Crystal structure of the dengue virus RNA-dependent RNA polymerase catalytic domain at 1 85-angstrom resolution. J. Virol. 81, 4753–4765.

You, S., Falgout, B., Markoff, L., Padmanabhan, R., 2001. In vitro RNA synthesis from exogenous dengue viral RNA templates requires long range interactions between 5′- and 3′-terminal regions that influence RNA structure. J. Biol. Chem. 276, 15581–15591.

You, S., Padmanabhan, R., 1999. A novel in vitro replication system for Dengue virus Initiation of RNA synthesis at the 3′-end of exogenous viral RNA templates requires 5′- and 3′-terminal complementary sequence motifs of the viral RNA. J. Biol. Chem. 274, 33714–33722.

Zeng, L., Falgout, B., Markoff, L., 1998. Identification of specific nucleotide sequences within the conserved 3′-SL in the dengue type 2 virus genome required for replication. J. Virol. 72, 7510–7522.

Zhong, W., Ferrari, E., Lesburg, C.A., Maag, D., Ghosh, S.K., Cameron, C.E., Lau, J.Y., Hong, Z., 2000. Template/primer requirements and single nucleotide incorporation by hepatitis C virus nonstructural protein 5B polymerase. J. Virol. 74, 9134–9143.